Application of Model-based Prognostics to a Pneumatic Valves Testbed

Matthew Daigle
NASA Ames Research Center
Moffett Field, CA 94035
matthew.j.daigle@nasa.gov

Chetan S. Kulkarni
SGT Inc., NASA Ames Research Center
Moffett Field, CA 94035
chetan.s.kulkarni@nasa.gov

George Gorospe
SGT Inc., NASA Ames Research Center
Moffett Field, CA 94035
george.e.gorospe@nasa.gov

Abstract— **Pneumatic-actuated valves play an important role in many applications, including cryogenic propellant loading for space operations. Model-based prognostics emphasizes the importance of a model that describes the nominal and faulty behavior of a system, and how faulty behavior progresses in time, causing the end of useful life of the system. We describe the construction of a testbed consisting of a pneumatic valve that allows the injection of faulty behavior and controllable fault progression. The valve opens discretely, and is controlled through a solenoid valve. Controllable leaks of pneumatic gas in the testbed are introduced through proportional valves, allowing the testing and validation of prognostics algorithms for pneumatic valves. A new valve prognostics approach is developed that estimates fault progression and predicts remaining life based only on valve timing measurements. Simulation experiments demonstrate and validate the approach.**

TABLE OF CONTENTS

1. INTRODUCTION

Pneumatic-actuated valves play a critical role in many systems. For example, in cryogenic propellant loading, these valves are used to control the flow of propellant, and failures may have a significant impact on launch availability [1]. There is thus a critical need for valve health monitoring and prognosis. In order to mature such approaches, testbeds can be used to inject faults in a controlled way, and validate valve prognosis algorithms. To fulfill this need, we have constructed a pneumatic valve testbed that satisfies these requirements [2].

In earlier work on valve prognosis [1, 3, 4], we developed methods for valve prognosis based on particle filtering. This approach, however, can be computationally intensive, and when measuring only valve position, as is the case in real valve operations, the only useful information is valve timing values, such as opening and closing times. In this paper, we develop a new approach that is much more efficient and requires only valve opening and closing times to isolate and identify faults, and predict end of life (EOL) and remaining useful life (RUL). The approach still follows the general estimation-prediction framework developed in the literature for model-based prognostics [5, 6]. We present simulation-based experiments that demonstrate the approach and investigate its sensitivity to noise in the valve timing values.

The structure of the paper is as follows. Section 2 discusses the overall setup of the valve prognostics testbed. Section 3 presents the valve model. Section 4 develops the valve prognosis framework, and Section 5 presents simulation-based prognosis results. Section 6 concludes the paper.

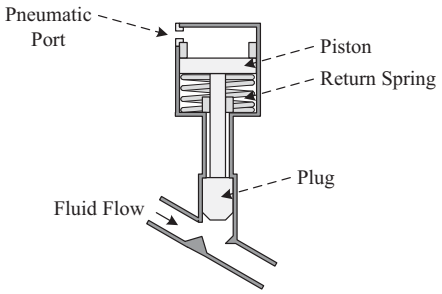

Figure 2. Discrete-controlled valve.

2. VALVE TESTBED

The prognostics demonstration testbed, shown in Fig. 1, has been developed to demonstrate valve prognosis in the context of cryogenic refueling operations. The dashed lines denote the electrical signals, including the data acquisition I/O signals, power lines, etc. The solid lines denote the pneumatic pressure lines connecting the supply and the valves. Power is provided by both a typical power supply and a battery backup supply, and includes a fail-safe mode to isolate the prognostics demonstration testbed from the cryogenic testbed on which it will be applied in the future.

The testbed includes a discrete-controlled valve (DV), illustrated in Fig. 2, which is a normally-open valve with a linear cylinder actuator. The valve is closed by filling the chamber above the piston with gas up to the supply pressure, and opened by evacuating the chamber to atmosphere, with the spring returning the valve to its default position.

A three-way two-position solenoid valve (SV), illustrated in

978-1-4799-1622-1/14/$31.00 ©2014 IEEE.
[1] IEEEAC Paper #2293, Version 2, Updated 12/01/2014.

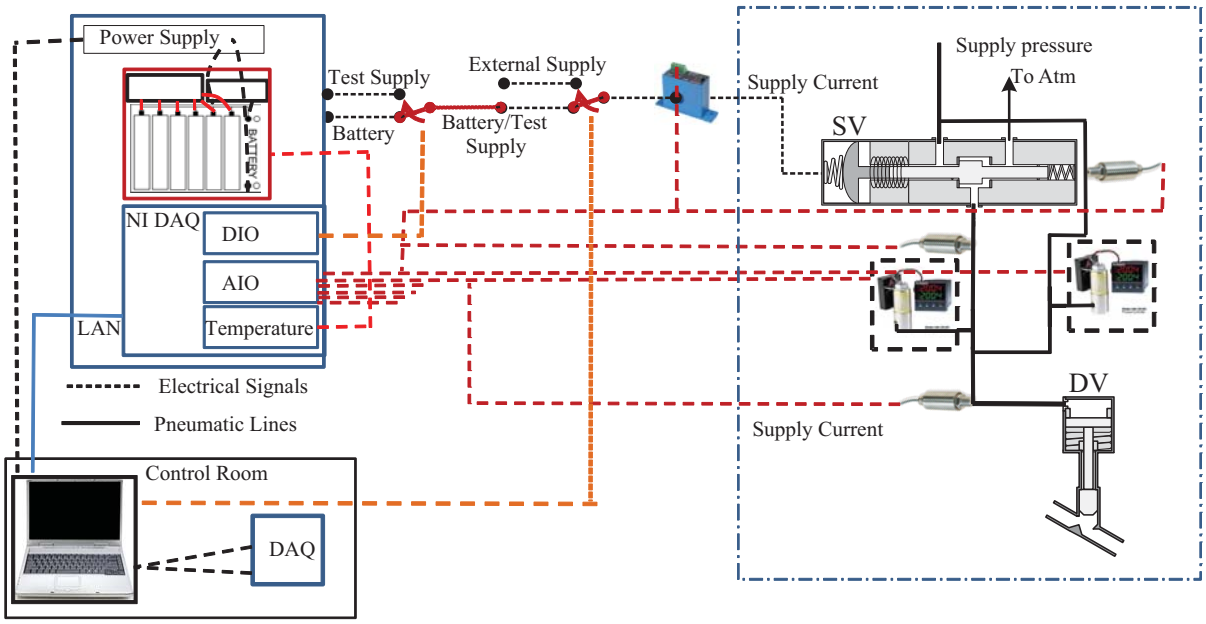

Figure 1. Prognostics demonstration testbed schematic.

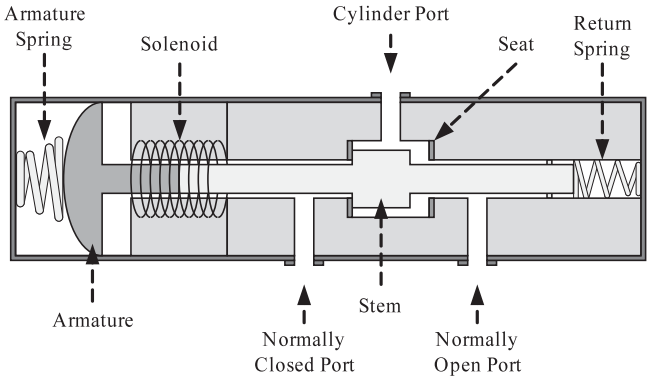

Figure 3. Three-way two-position solenoid valve.

Fig. 3, is used for controlling the operation of the DV valve. The cylinder port connects to the valve, the normally closed (NC) port connects to the supply pressure, and normally open (NO) port is left unconnected, allowing venting to atmosphere. When the solenoid is energized, the path from the NC port to cylinder port is open, allowing gas to pass from the supply to the valve, thus actuating the valve. When deenergized, the supply pressure is closed off and the path from the cylinder port to the NO port is opened, thus venting the DV valve which opens the valve due to the return spring. The solenoid is powered by 24 V dc either through the power supply or the batteries.

As part of a backup power supply source, Li-ion batteries are used for powering the solenoid valve. Each cell has a voltage of around 4.2 V when fully charged. The terminal voltage of the battery rises/falls with a charge/discharge cycle, respectively. In order to obtain a total dc voltage of around 24 V to operate the solenoid, we connect 6 batteries in series.

The data from the different sensors is collected using an 8-slot NI cDAQ-9188 Gigabit Ethernet chassis as the data acquisition (DAQ) system that is designed for remote or distributed sensor measurements. For the experimental testbed, control and data acquisition must be done remotely to meet safety requirements. A single NI CompactDAQ chassis can measure up to 256 channels of sensor signals, analog I/O, digital I/O, and counter/timers with an Ethernet interface back to a host machine. All the operations for the cDAQ-9188 are controlled through an interface designed in LabVIEW. Additional details of the testbed and data aquisition system are described in [2].

With the testbed, we can investigate solenoid valve prognostics [7], battery prognostics [8], and pneumatic valve prognostics [1]. In this work, we focus on faults affecting the pneumatic valves. Pneumatic valves can suffer from leaks, increase in friction due to wear, and spring degradation [1]. Friction and spring faults cannot be injected or their rate of progression controlled, so we are limited only to leak faults, which, in any case, are the most common faults. In the configuration shown in Fig. 1, two different leak faults may be considered: (*i*) a leak to atmosphere, and (*ii*) a leak from the supply. In the former, this can manifest as a leak across the NO seat of the solenoid valve, or a leak on the gas line going to the pneumatic valve. In the latter case, the fault can manifest as a leak across the NC seat of the solenoid valve. To emulate these faults, we install two remotely-operated proportional valves, as shown in Fig. 1. One valve leaks to atmosphere (henceforth called the vent valve), while the other is installed on a bypass line around the solenoid valve (henceforth called the bypass valve).

The leak valves combine a solenoid valve with an electronics package that digitally modulates the control signal to provide analog proportional control. They are two-way normally-closed valves and operate on 24 V dc, powered through the power supply or the batteries. The leak valves allow control over how much they can be opened in order to control the leakage rate and support desired damage progression profiles.

Fig. 5 illustrates for a leak to atmosphere, using a vent valve V1. The leak through V1 emulates a leak at the cylinder port or across the NO seat. Similarly, Fig. 4 illustrates the setup

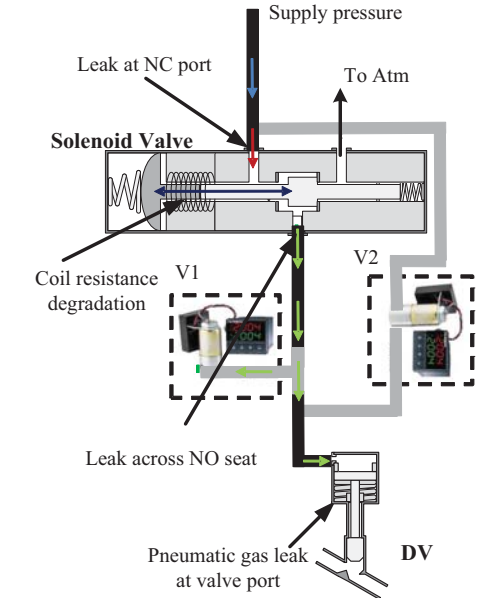

Figure 4. Solenoid valve leak fault injection when energized on DV valve.

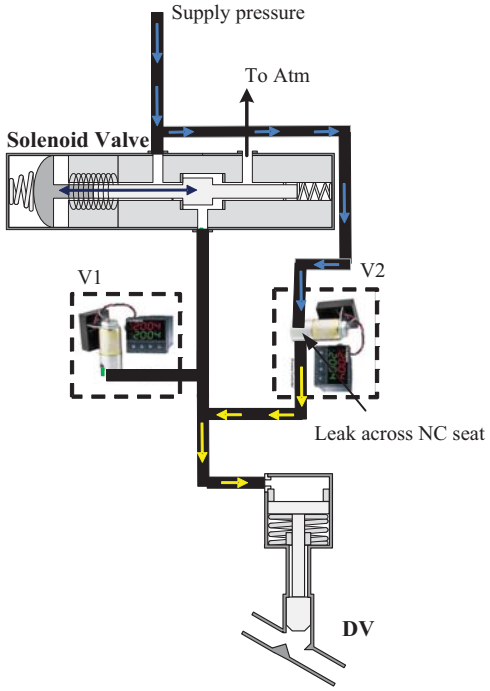

Figure 5. Solenoid valve leak fault injection when de-energized on DV valve.

for a leak from the supply, using a bypass valve V2. The leak through V2 emulates a leak across the NC seat. The effect of these faults on valve behavior will be described in Section 3.

3. VALVE MODELING

We consider here a normally-open valve with a linear cylinder actuator, shown in Fig. 2. The valve is opened by filling the chamber above the piston with pneumatic gas up to the supply pressure. The valve is closed by evacuating the gas to atmosphere, with the return spring forcing the valve back to its default position. We present here the model using continuous-time. For implementation purposes, we convert to a discrete-time version using a sample time of 1×10^{-3} s.

We develop a physics model of the valve based on mass and energy balances. The system state includes the position of the valve, $x(t)$, the velocity of the valve, $v(t)$, the mass of the gas in the volume above the piston, and the mass of the gas in the pipe connecting the solenoid valve to the pneumatic valve port:

$$\mathbf{x}(t) = [x(t) \quad v(t) \quad m_t(t) \quad m_p(t)]^T .$$

The position is defined as $x = 0$ when the valve is fully closed, and $x = L_s$ when fully open, where L_s is the stroke length of the valve.

The derivatives of the states are described by

$$\dot{\mathbf{x}}(t) = [v(t) \quad a(t) \quad f_t(t) \quad f_p(t)]^T ,$$

where $a(t)$ is the valve acceleration, $f_t(t)$ is the mass flow going into the pneumatic port from the pipe, and $f_p(t)$ is the total mass flow into the pipe.

The single input is considered to be

$$\mathbf{u}(t) = [u_t(t)] ,$$

where $u_t(t)$ is input pressures to pneumatic port, which alternates between the supply pressure and atmospheric pressure depending on the commanded valve position.

The acceleration is defined by the combined mass of the piston and plug, m, and the sum of forces acting on the valve, which includes the force from the pneumatic gas, $F_p = (p_t(t) - p_{atm})A_p$, where $p_t(t)$ is the gas pressures on the top of the piston, and A_p is the surface area of the piston; the weight of the moving parts of the valve, $F_w = -mg$, where g is the acceleration due to gravity; the spring force, $F_s = k(x(t) + x_o)$, where k is the spring constant and x_o is the amount of spring compression when the valve is open; friction, $F_f = -rv(t)$, where r is the coefficient of kinetic friction, and the contact forces $F_c(t)$ at the boundaries of the valve motion,

$$F_c(t) = \begin{cases} k_c(-x), & \text{if } x < 0, \\ 0, & \text{if } 0 \le x \le L_s, \\ -k_c(x - L_s), & \text{if } x > L_s, \end{cases}$$

where k_c is the (large) spring constant associated with the flexible seals. Overall, the acceleration term is defined by

$$a(t) = \frac{1}{m}(F_s - F_p - F_f - F_w + F_c)$$

The pressure $p_t(t)$ and the pipe pressure, $p_p(t)$, are calculated as:

$$p_t(t) = \frac{m_t(t)R_gT}{V_{t_0} + A_p(L_s - x(t))} \qquad p_p(t) = \frac{m_p(t)R_gT}{V_p}$$

where we assume an isothermal process in which the (ideal) gas temperature is constant at T, R_g is the gas constant for

the pneumatic gas, V_{t_0} is the minimum gas volume for the gas chamber above the piston, and V_p is the pipe volume.

The gas flows are given by:

$$\begin{aligned} f_{p,in}(t) &= f_g(u_t(t), p_p(t)) \\ f_{p,leak}(t) &= f_g(p_p(t), p_{leak}) \\ f_{p,t}(t) &= f_g(p_p(t), p_t(t)) \\ f_p(t) &= f_{p,in}(t) - f_{p,t}(t) - f_{p,leak}(t) \\ f_t(t) &= f_{p,t}(t) \end{aligned}$$

where $f_{p,in}$ is the flow into the pipe from the supply or atmosphere, $f_{p,leak}$ is a leak term with p_{leak} being the pressure outside the leak, $f_{p,t}$ is the flow from the pipe to the chamber above the piston, and f_g defines gas flow through an orifice for choked and non-choked flow conditions [9]. Non-choked flow for $p_1 \geq p_2$ is given by $f_{g,nc}(p_1, p_2) =$

$$C_s A_s p_1 \sqrt{\frac{\gamma}{Z R_g T}\left(\frac{2}{\gamma-1}\right)\left(\left(\frac{p_2}{p_1}\right)^{\frac{2}{\gamma}} - \left(\frac{p_2}{p_1}\right)^{\frac{\gamma+1}{\gamma}}\right)},$$

where γ is the ratio of specific heats, Z is the gas compressibility factor, C_s is the flow coefficient, and A_s is the orifice area. Choked flow for $p_1 \geq p_2$ is given by

$$f_{g,c}(p_1, p_2) = C_s A_s p_1 \sqrt{\frac{\gamma}{Z R_g T}\left(\frac{2}{\gamma+1}\right)^{\frac{\gamma+1}{\gamma-1}}}.$$

Choked flow occurs when the upstream to downstream pressure ratio exceeds $\left(\frac{\gamma+1}{2}\right)^{\gamma/(\gamma-1)}$. The overall gas flow equation is then given by

$$f_g(p_1, p_2) = \begin{cases} f_{g,nc}(p_1, p_2) & \text{if } p_1 \geq p_2 \\ & \text{and } \frac{p_1}{p_2} < \left(\frac{\gamma+1}{2}\right)^{\frac{\gamma}{(\gamma-1)}}, \\ f_{g,c}(p_1, p_2) & \text{if } p_1 \geq p_2 \\ & \text{and } \frac{p_1}{p_2} \geq \left(\frac{\gamma+1}{2}\right)^{\frac{\gamma}{(\gamma-1)}}, \\ -f_{g,nc}(p_2, p_1) & \text{if } p_2 > p_1 \\ & \text{and } \frac{p_2}{p_1} < \left(\frac{\gamma+1}{2}\right)^{\frac{\gamma}{(\gamma-1)}}, \\ -f_{g,c}(p_2, p_1) & \text{if } p_2 > p_1 \\ & \text{and } \frac{p_2}{p_1} \geq \left(\frac{\gamma+1}{2}\right)^{\frac{\gamma}{(\gamma-1)}}, \end{cases}.$$

The only available measurement is the valve position, so we have

$$\mathbf{y}(t) = [x(t)].$$

Fig. 6 shows a nominal valve cycle. The valve starts in its default open state. The valve is commanded to close at 0 s. Supply pressure (75 psig) is delivered to the pipe and to the valve, causing the piston to lower, closing the valve just after 1 s. At 4 s, the valve is commanded to open, and the pipe is opened to atmosphere. The pipe pressure and valve pressure drop, and once the pressure drops low enough, the spring overcomes the pressure force and the piston moves updwards. The valve completes opening just after 6 s. The valve parameters were identified from known valve specifications, and unknown parameters estimated to match the nominal opening and closing times.

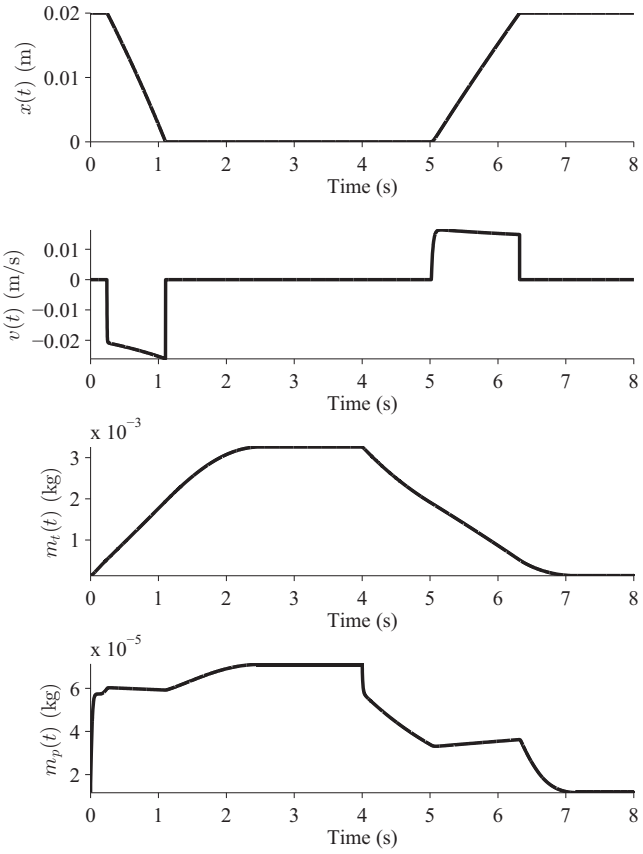

Figure 6. Nominal valve operation.

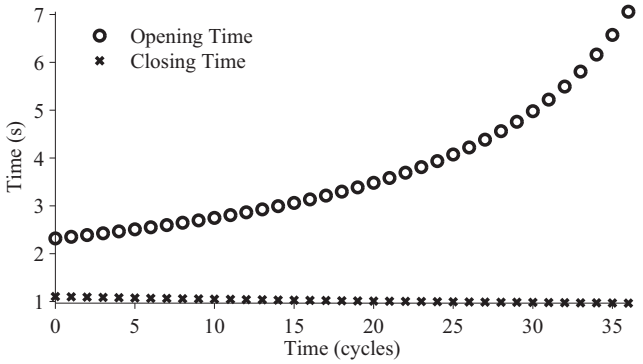

Figure 7. Valve timing with leak from supply, with linearly increasing leak area.

As discussed in Section 2, we consider two different leak faults, one in which there is a leak from the supply pressure input to the valve (p_{leak} is the supply pressure), emulated using the bypass valve, and one in which there is a leak out to atmosphere (p_{leak} is atmospheric pressure), emulated using the vent valve. In the former case, the valve will close more slowly and open faster, and in the latter, the valve will open more slowly and close faster. With a large enough leak, the valve may fail to open or close fully. Fig. 7 shows the changes in valve timing with the leak from the supply, and Fig. 8 shows the changes in valve timing with the leak to atmosphere. Here, we consider a damage progression model where the leak hole area increases linearly with time.

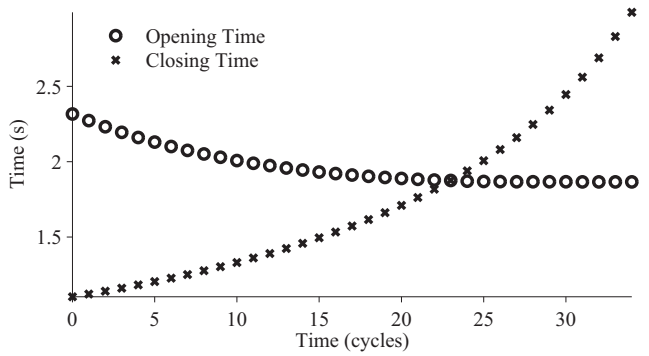

Figure 8. Valve timing with leak to atmosphere, with linearly increasing leak area.

We define end of life through the use of timing limits on the valves, as is done in real valve operations [1]. The valve in the testbed is required to open within 6 s and close within 3 s.

4. VALVE PROGNOSIS

We describe in this section the prognosis framework developed for the valve. We follow here the same general estimation-prediction framework of model-based prognostics [5, 6, 10]. However, since we use only valve timing values for prognosis, we use a simpler estimation approach, similar to that developed in [11], as opposed to more complex and computationally intensive filtering approaches used in previous works. We first formulate the prognostics problem, followed by a description of the estimation approach and a description of the prediction approach.

Problem Formulation

We assume the system model may be generally defined as

$$\mathbf{x}(k+1) = \mathbf{f}(k, \mathbf{x}(k), \boldsymbol{\theta}(k), \mathbf{u}(k), \mathbf{v}(k)),$$
$$\mathbf{y}(k) = \mathbf{h}(k, \mathbf{x}(k), \boldsymbol{\theta}(k), \mathbf{u}(k), \mathbf{n}(k)),$$

where k is the discrete time variable, $\mathbf{x}(k) \in \mathbb{R}^{n_x}$ is the state vector, $\boldsymbol{\theta}(k) \in \mathbb{R}^{n_\theta}$ is the unknown parameter vector, $\mathbf{u}(\mathbf{k}) \in \mathbb{R}^{\mathbf{n_u}}$ is the input vector, $\mathbf{v}(k) \in \mathbb{R}^{n_v}$ is the process noise vector, $\mathbf{f}$ is the state equation, $\mathbf{y}(k) \in \mathbb{R}^{n_y}$ is the output vector, $\mathbf{n}(k) \in \mathbb{R}^{n_n}$ is the measurement noise vector, and $\mathbf{h}$ is the output equation.[2]

In prognostics, we are interested in predicting the occurrence of some event E that is defined with respect to the states, parameters, and inputs of the system. We define the event as the earliest instant that some event threshold $T_E : \mathbb{R}^{n_x} \times \mathbb{R}^{n_\theta} \times \mathbb{R}^{n_u} \rightarrow \mathbb{B}$, where $\mathbb{B} \triangleq \{0, 1\}$ changes from the value 0 to 1 [12]. That is, the time of the event k_E at some time of prediction k_P is defined as

$$k_E(k_P) \triangleq \inf\{k \in \mathbb{N} \colon k \geq k_P \wedge T_E(\mathbf{x}(k), \boldsymbol{\theta}(k), \mathbf{u}(k)) = 1\}.$$

The time remaining until that event, Δk_E, is defined as

$$\Delta k_E(k_P) \triangleq k_E(k_P) - k_P.$$

In the context of systems health management, T_E is defined via a set of performance constraints that define what the acceptable states of the system are, based on $\mathbf{x}(k)$, $\boldsymbol{\theta}(k)$, and $\mathbf{u}(k)$ [6]. In this context, k_E represents end of life (EOL), and Δk_E represents remaining useful life (RUL). For valves, timing requirements are provided that define the maximum allowable time a valve may take to open or close, and these define T_{EOL} [1].

The prognostics problem is to compute estimates of EOL and/or RUL. To do this, we first perform an estimation step that computes estimates of $\mathbf{x}(k)$ and $\boldsymbol{\theta}(k)$, followed by a prediction step that computes EOL/RUL using these values as initial states. For the case of the valve, the future inputs are known, i.e., the valve is simply cycled open and closed, so there is no uncertainty with respect to future inputs.

Estimation

Since only valve position is measured, only valve timing values are useful for prognostics. We can extract from the continous position measurement this information, by computing the difference in time between when the valve is commanded to move, and when it reaches its final position. Using the model, we can search for the leak parameter value that matches the observed opening or closing time. We can do this using an optimization routine. We provide the observed timing value and an initial guess of the leak size. The algorithm then tries different parameter values to try to minimize the error between predicted valve timing (via simulating the model) and observed valve timing. We use the standard Nedler-Mead simplex algorithm for this purpose. Another method is to build a lookup table mapping leak size to open and close times, using the simulation model [11]. With a fine enough granularity, a lookup table will provide the same results as the optimization routine but at a fraction of the computational cost. To estimate the parameter that defines how the fault evolves in time, we assume a linear progression of the leak parameter and perform a linear regression on the history of estimated leak parameters.

For the leak to atmosphere, only closing times can be used. This is because, in the presence of this leak, the valve may not get up to the full supply pressure when the valve closes in time for the next cycle, so since the internal valve actuator pressure is not measured, we do not have a correct initial condition for the simulation with which to estimate the leak parameter value for the following opening time. For the supply leak, we have analogous situation and can use only opening times for leak parameter estimation.

Prediction

Given the current estimated leak parameter value, and the regression parameters, we can compute the value of the leak parameter at any future time, defining the damage progression equation. Given the maximum leak parameter value corresponding to valve EOL, we can solve for the time at which this occurs using the determined damage progression equation.

We can isolate which fault is present by inspecting the associated predictions. If we assume a supply leak is present, but the leak is to atmosphere (or vice versa), the estimated leak parameter values will decrease in time and the EOL and RUL values will be nonsensical.

[2]Bold typeface denotes vectors, and n_a denotes the length of a vector $\mathbf{a}$.

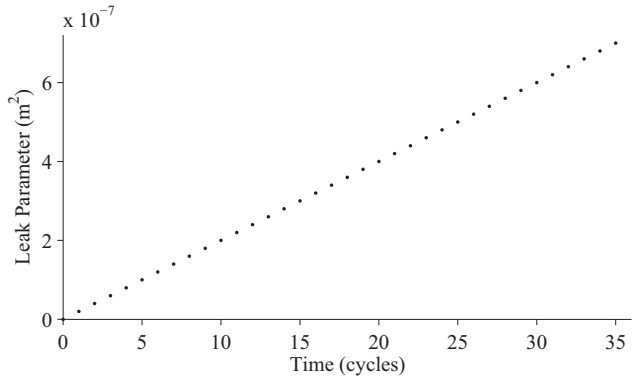

Figure 9. Leak parameter estimation for a leak from supply, based on valve opening times, in the noise-free case.

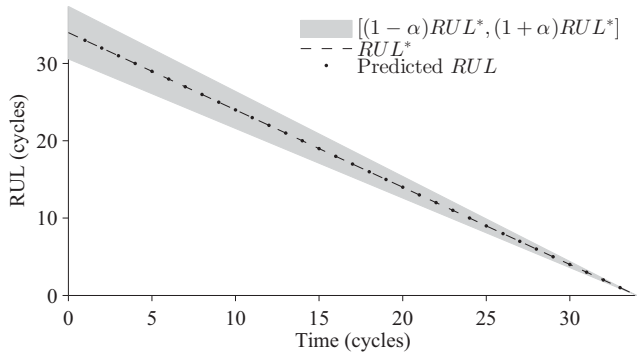

Figure 10. RUL predictions for a leak from supply, in the noise-free case.

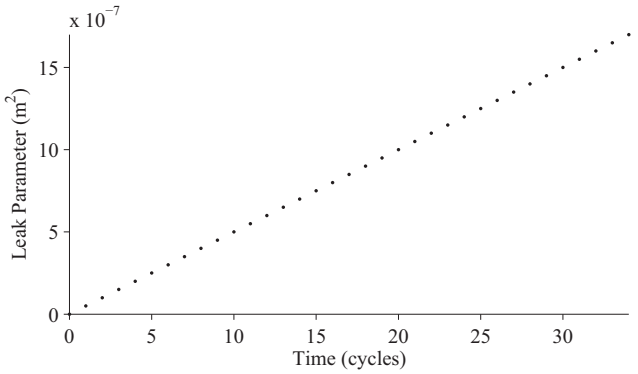

Figure 11. Leak parameter estimation for a leak to atmosphere, based on valve closing times, in the noise-free case.

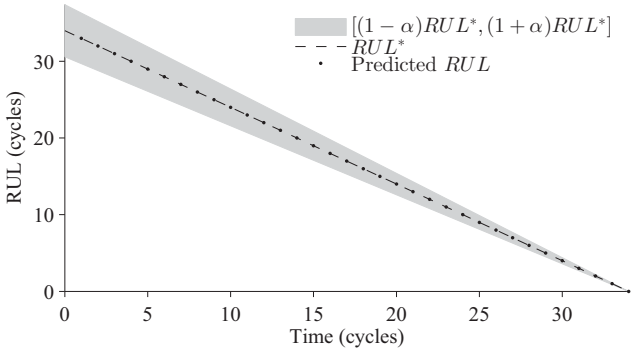

Figure 12. RUL predictions for a leak to atmosphere, in the noise-free case.

5. RESULTS

We consider the case where the valve is cycled repeatedly, and the leak hole area (controlled by the open percentage of the leak valve) is slowly increasing linearly with time. We begin with the ideal case in which there is no noise and so valve opening and closing times can be acquired precisely. Fig. 9 shows the estimated leak parameter after each cycle for a leak from the supply. Based on the opening times, the leak parameter can be estimated very accurately, since the model is very accurate. Fig. 10 shows the RUL predictions after each cycle (rounded to the nearest cycle), where $\alpha = 0.1$ represents a desired accuracy constraint, and RUL^* denotes the true RUL. Convergence occurs quickly, and accurate EOL predictions are available after only two cycles. Relative accuracy is 100% averaged over all predictions, since the model is known exactly and there is no noise. This represents the ideal case.

Similar results are obtained for the leak to atmosphere. Accurate estimation results are achieved, as shown in Fig. 11, as well as accurate predictions Fig. 12. Again, this represents the ideal case.

We consider now the case where sensor and model noise are present, resulting in noisy computations of valve opening and closing times. We assume a noise variance on the timing values of 1×10^{-3}. Fig. 13 shows the measured valve timing values for a leak from supply. Fig. 14 shows the associated estimated leak parameter values, and Fig. 15 shows the RUL predictions. Results are clearly less accurate in the presence of noise. Leak parameter estimation loses accuracy due to noisy timing values, and, as a result, RUL predictions take longer to converge. Here, relative accuracy for the RUL predictions averages to 79.6%, and estimates converge only after 7 cycles; after that point, relative accuracy improves to 86.0%.

Fig. 16 shows the measured valve timing values for a leak to atmosphere. Fig. 17 shows the associated estimated leak parameter values, and Fig. 18 shows the RUL predictions. Results here are also less accurate in the presence of noise. Here, relative accuracy for the RUL predictions averages to 79.9%, and estimates converge only after 8 cycles; after that point, relative accuracy improves significantly to 97.6%.

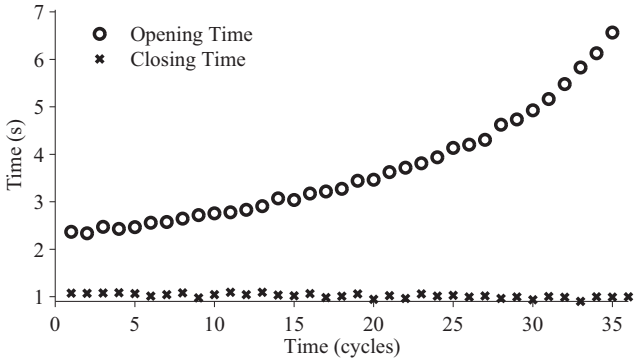

Figure 13. Valve open and close times for a leak from supply, with noise.

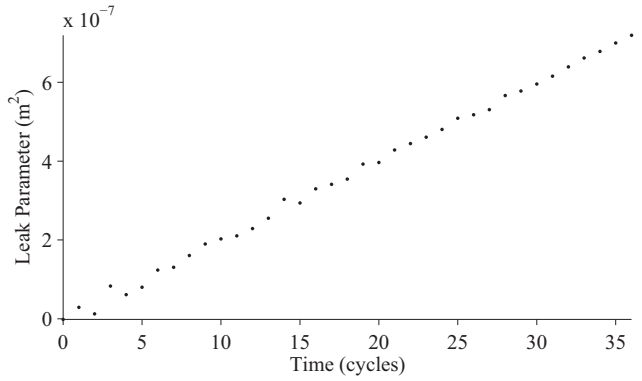

Figure 14. Leak parameter estimation for a leak from supply, based on valve opening times.

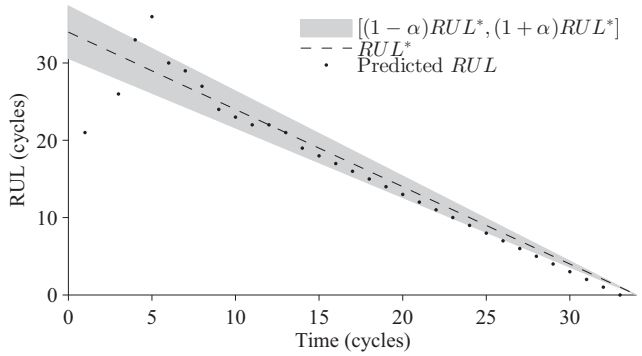

Figure 15. RUL predictions for a leak from supply.

With an order of magnitude less noise variance, relative accuracy becomes 96.5% for the leak from supply fault, converging after 5 cycles after which relative accuracy improves to 98.5%. For the leak to atmosphere, relative accuracy becomes 95.3% for the leak from supply fault, converging after 3 cycles after which relative accuracy improves to 96.8%. For an order of magnitude more noise, average relative accuracy reduces to 31.4% for the supply leak, never converging to within 10% of the true value. For the leak to atmosphere, average relative accuracy reduces to 34.4% with convergence in 23 cycles, after which relative accuracy improves to 97.7%. This analysis demonstrates the sensitivity of the approach to noise in the timing values and stresses the importance of accurate calculation of these values. Of course, with a more slowly progressing fault, more data points will be available and the estimates should be able to converge much faster relative to the EOL value.

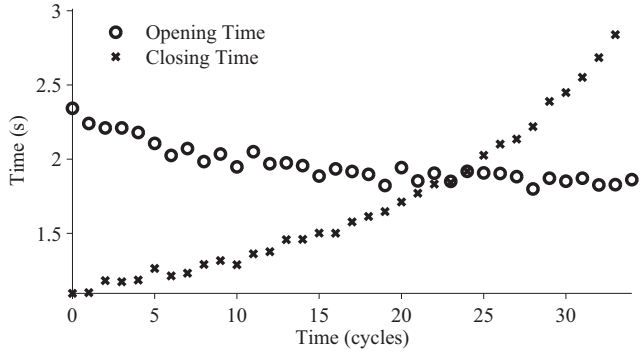

Figure 16. Valve open and close times for a leak to atmosphere, with noise.

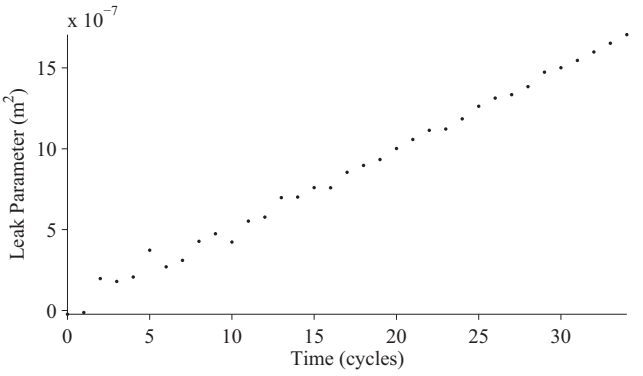

Figure 17. Leak parameter estimation for a leak to atmosphere, based on valve closing times, in the noise-free case.

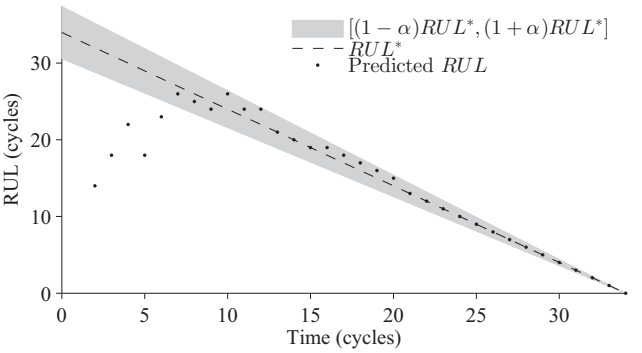

Figure 18. RUL predictions for a leak to atmosphere, in the noise-free case.

6. CONCLUSIONS

In this paper, we described a testbed for injecting faults in pneumatic valves. We developed a model of the valve including leak faults, and presented a novel valve prognosis framework that operates with limited measurements, using only valve timing information for prognosis. We demonstrated the approach in simulation, and analyzed the robustness of the approach with different noise values.

Future work will involve validating the prognosis framework with experimental data from the testbed, and applying the approach to a second type of valve that is continuously controlled.

ACKNOWLEDGMENTS

This work was funded in part by the NASA Automated Cryogenic Loading Operations (ACLO) project under the Office of the Chief Technologist (OCT) and the Advanced Ground Systems Maintenance (AGSM) Project under the Ground Systems Development and Operations (GSDO) Program.

REFERENCES

[1] M. Daigle and K. Goebel, "A model-based prognostics approach applied to pneumatic valves," *International Journal of Prognostics and Health Management*, vol. 2, no. 2, Aug. 2011.

[2] C. Kulkarni, M. Daigle, and K. Goebel, "Implementation of prognostic methodologies to cryogenic propellant loading testbed," in *IEEE AUTOTESTCON 2013*, Sep. 2013.

[3] M. Daigle and K. Goebel, "Prognostics for ground support systems: Case study on pneumatic valves," in *Proceedings of AIAA Infotech@Aerospace 2011 Conference*, Mar. 2011.

[4] ——, "Model-based prognostics under limited sensing," in *2010 IEEE Aerospace Conference*, Mar. 2010.

[5] M. Orchard and G. Vachtsevanos, "A particle filtering approach for on-line fault diagnosis and failure prognosis," *Transactions of the Institute of Measurement and Control*, no. 3-4, pp. 221–246, Jun. 2009.

[6] M. Daigle and K. Goebel, "Model-based prognostics with concurrent damage progression processes," *IEEE Transactions on Systems, Man, and Cybernetics: Systems*, vol. 43, no. 4, pp. 535–546, May 2013.

[7] ——, "Improving computational efficiency of prediction in model-based prognostics using the unscented transform," in *Proc. of the Annual Conference of the Prognostics and Health Management Society 2010*, Oct. 2010.

[8] M. Daigle and C. Kulkarni, "Electrochemistry-based battery modeling for prognostics," in *Annual Conference of the Prognostics and Health Management Society 2013*, Oct. 2013, pp. 249–261.

[9] R. Perry and D. Green, *Perry's chemical engineers' handbook*. McGraw-Hill Professional, 2007.

[10] J. Luo, K. R. Pattipati, L. Qiao, and S. Chigusa, "Model-based prognostic techniques applied to a suspension system," *IEEE Transactions on Systems, Man and Cybernetics, Part A: Systems and Humans*, vol. 38, no. 5, pp. 1156 –1168, Sep. 2008.

[11] C. Teubert and M. Daigle, "I/P transducer application of model-based wear detection and estimation using steady state conditions," in *Proceedings of the Annual Conference of the Prognostics and Health Management Society 2013*, Oct. 2013, pp. 134–140.

[12] M. Daigle and S. Sankararaman, "Advanced methods for determining prediction uncertainty in model-based prognostics with application to planetary rovers," in *Annual Conference of the Prognostics and Health Management Society 2013*, Oct. 2013, pp. 262–274.

Matthew Daigle *received the B.S. degree in Computer Science and Computer and Systems Engineering from Rensselaer Polytechnic Institute, Troy, NY, in 2004, and the M.S. and Ph.D. degrees in Computer Science from Vanderbilt University, Nashville, TN, in 2006 and 2008, respectively. From September 2004 to May 2008, he was a Graduate Research Assistant with the Institute for Software Integrated Systems and Department of Electrical Engineering and Computer Science, Vanderbilt University, Nashville, TN. From June 2008 to December 2011, he was an Associate Scientist with the University of California, Santa Cruz, at NASA Ames Research Center. Since January 2012, he has been with NASA Ames Research Center as a Research Computer Scientist. His current research interests include physics-based modeling, model-based diagnosis and prognosis, simulation, and hybrid systems. Dr. Daigle is a member of the Prognostics and Health Management Society and the IEEE.*

Chetan S. Kulkarni *received the B.E. degree in Electronics and Electrical Engineering from University of Pune, India in 2002 and the M.S. and Ph.D. degrees in Electrical Engineering from Vanderbilt University, Nashville, TN, in 2009 and 2013, respectively. In 2002 he joined Honeywell Automation India Limited (HAIL) as a Project Engineer. From May 2006 to August 2007 he was a Research Fellow at the Indian Institute of Technology (IIT) Bombay with the Department of Electrical Engineering. From Aug 2007 to Dec 2012, he was a Graduate Research Assistant with the Institute for Software Integrated Systems and Department of Electrical Engineering and Computer Science, Vanderbilt University, Nashville, TN. Since January 2013 he has been a Research Engineer II with SGT Inc. at the Prognostics Center of Excellence, NASA Ames Research Center. His current research interests include physics-based modeling, model-based diagnosis and prognosis focused towards electrical and electronic devices and systems. Dr. Kulkarni is a member of the Prognostics and Health Management (PHM) Society, AIAA and the IEEE.*

George Gorospe *received the B.E. degree in Mechanical Engineering from the University of New Mexico, Albuquerque, New Mexico, USA, in 2012. Since October 2012, he has been a research engineer with the NASA Ames Research Center. His current research interests include mission design, systems engineering, and autonomous mobile robot control and control systems engineering.*